Materials Science in Semiconductor Processing 75 (2018) 166–172

Contents lists available at ScienceDirect

Materials Science in Semiconductor Processing

journal homepage: www.elsevier.com/locate/mssp

Effect of post-annealing on the properties of thermally evaporated molybdenum oxide films: Interdependence of work function and oxygen to molybdenum ratio

Baichao Han[a], Ming Gao[a], Yazhou Wan[a], Yong Li[a], Wenlei Song[a], Zhongquan Ma[a,b,*]

[a] SHU-SOEN's R&D Lab, Department of Physics, Shanghai University, Shanghai 200444, China
[b] Instrumental Analysis & Research Center, Shanghai University, Shanghai 200444, China

ARTICLE INFO

Keywords:
Molybdenum oxide
Thermal evaporation
O/Mo ratio
Work function
Optical properties

ABSTRACT

Molybdenum oxide (MoO_x, $x < 3$) thin films were deposited on glass and (100) silicon substrates by thermal evaporation technique. Post-annealing of the samples was performed in O_2 by rapid thermal process at 373–673 K. The surface chemical, structural , morphological and optical properties of the samples were investigated. X-ray photoelectron spectra characterization verified the growth of sub-stoichiometric MoO_x films as the coexistence of oxidation states of Mo^{6+} and Mo^{5+}. The O/Mo ratio of MoO_x films increases from 2.58 to 2.75 when the annealing temperature increases to 473 K, but this ratio rapidly decreases at higher temperatures. The work function of MoO_x films is proportional to O/Mo ratio and within the range of 5.40–5.95 eV. This correlation can be ascribed to the variation of Fermi level and surface dipole with oxygen vacancy. The MoO_x films are polycrystalline with nanoparticles, and both α- and β-phase MoO_3 are co-existed with the annealing temperature from 373 K to 673 K. The optical band gap of MoO_x films is in the scope of 2.72–2.95 eV. The three critical properties of MoO_x films, such as work function, optical band gap and transmittance, are well-correlated to the variation of chemical configuration with the annealing temperature.

1. Introduction

MoO_x thin films have attracted a great attention because of their wide application in charge-transfer fields, such as gas sensors [1,2], electrochromic devices [3,4], selective oxidation catalysis [5], and silicon heterojunction solar cells [6–12]. For the multi-functional thin films, various fabrication techniques have been employed to fabricate MoO_x films, including sol-gel processing [2], atomic layer deposition [12], chemical vapor deposition [13,14], sputtering [15–18], and thermal evaporation [6–11]. Among them, vacuum evaporation is the dominant method to fabricate MoO_x films and enables MoO_x widely applied in electrical and optical devices since this technique has the advantages of low cost, high efficiency and minor damage to substrate. Besides, the melting point of MoO_3 is only 795 °C, which can be easily gasified in a low-pressure chamber [19]. Especially, the work function (W_F) of stoichiometric MoO_3 is as high as to 6.9 eV, and the oxygen vacancy allow MoO_x ($2 < x < 3$) easily become a degenerate n-type semiconductor [19–21]. The wide band gap (3.0–3.3 eV) of MoO_3 make it high transparent in the visible region [7,8]. Additionally, it is reported that MoO_3 has a crystalline symmetry of monoclinic or orthorhombic structure, where the orthorhombic structure is more stable form and its layered structure is very suitable for the embedment of other small molecules or ions [11–14].

Recent years, the higher energy conversion efficiency of crystalline silicon (c-Si) solar cells was gradually created by silicon heterojunction (SHJ) technology and the record is up to 26.3% [22]. In the conventional SHJ solar cells, a thin intrinsic hydrogenated amorphous silicon layer (a-Si:H(i)) is used as an interface passivation layer for the c-Si wafer while p and n-type amorphous silicon layers [a-Si:H(p); a-Si:H (n)] serve as hole and electron collection layers at front and rear sides. However, the narrow band gap of (doped) a-Si:H with only about 1.6–1.8 eV and the high defect density in these layers would cause parasite absorption in the blue region [6,8]. Besides, a limitation by "narrow art-technique window" during the fabrication of the intrinsic or doped hydrogenated amorphous silicon thin films in a complex plasma enhanced chemical vapor deposition (PECVD) is another issue [23].

MoO_x, in particular, with high photon transmittance and carrier mobility can be a promising candidate as a window layer in SHJ solar cells. What's more, the high work function of MoO_x films could bring about a big work function difference ($\Phi_{MoO_x} - \Phi_{Si}$) with silicon substrate , which is also critical for the built-in electric potential difference

* Corresponding author at: SHU-SOEN's R&D Lab, Department of Physics, Shanghai University, Shanghai 200444, China.
E-mail address: zqma@t.shu.edu.cn (Z. Ma).

https://doi.org/10.1016/j.mssp.2017.11.037
Received 12 August 2017; Received in revised form 22 October 2017; Accepted 26 November 2017

and the holes collection [6–12,19–21]. Replacing the a-Si:H(p) with MoO_x layer, the conversion efficiency of SHJ solar cell is up to 22.5% [6]. However, the measured work function of MoO_x used in c-Si solar cell is only about 5.7 eV [7]. Further enhancing the work function of MoO_x would be significant for its application in c-Si solar cells.

Motivated by these investigations, in this research, we prepared MoO_x thin films via thermal evaporation and then these samples undergone post-annealing. The influence of the different annealing temperatures on the surface chemical, structural and optical characteristics of the samples were investigated.

2. Experimental in details

Molybdenum oxide films were deposited on cleaned glass and (100) silicon substrates by thermal evaporation of high-quality MoO_3 power (99.9% purity, Alfa Aesar) from a Mo boat. The distance between the source and substrate was fixed to 26 cm and the base pressure of the chamber was about 4×10^{-5} mbar. Prior to deposition of MoO_x thin films, the substrates were cleaned by a standard cleaning method [24]. During the process of deposition, the current on the Mo boat was maintained at 100 A. Post-deposition annealing was done at 373–673 K for 30 min in O_2 ambience, using a programmed rapid thermal furnace. The flow rate of high purity oxygen was 0.6 L/min. The MoO_x film thicknesses measured via profiler-system (Ambios XP-200) were all about 160 nm.

The electronic binding energy and the chemical oxidation states of the samples were examined by XPS (Thermo Fisher Scientific Model ESCA-250Xi). In order to eliminate the influence of adsorbed oxygen, the films were etched by Ar^+ ion beam with 500 eV for 5 s. A monochromatic Al kα excitation source ~ 1486.6 eV was employed for the XPS measurements. The pass energy, scan step, and test area were set to be 30.00 eV, 0.10 eV and 500 μm × 500 μm, respectively. The work function of the MoO_x films were evaluated by UPS with He I excitation line (21.22 eV). The UPS measurement offers an energy resolution of 0.09 eV. Structural properties of the samples were investigated by X-Ray Diffraction (XRD, 18 kW D/MAX2500V + /PC). Raman spectra were obtained by confocal microscopic Raman spectrometer (NTEGRA Spectra II) with the laser excitation source at 532 nm. SEM images were acquired using a JSM-7500F Camera. The optical transmittance was recorded within the range of 300–900 nm via TU1901 UV–VIS spectrophotometer.

3. Results and discussion

3.1. Surface chemical states

The XPS studies give the information about the electronic binding energies and oxidation states in the MoO_x films. The XPS spectra of MoO_x films, without annealing treatment or annealed at different temperatures, show the characteristic peaks of MoO_3. Fig. 1 shows a representative XPS spectrum of the as-deposited MoO_x film. The weak C 1s peak at around 284.88 eV is a result of carbon contamination since the films were exposed to air. Moreover, other peaks were also identified and their binding energies are listed in Table 1 [15,16].

XPS spectra of Mo 3d doublets of MoO_x films annealed at various temperatures are presented in Fig. 2, and their binding energies are summarized in Table 2. All patterns show slightly asymmetric peaks, illustrating both the existence of mixed oxidation states of Mo and the growth of sub-stoichiometric films [15,16]. The peak fitting presented in Fig. 2 indicated that all the samples included two oxidation states of Mo^{6+} and Mo^{5+}. The oxidation state of Mo^{4+} would have lower binding energy and was not detected here [25]. The binding energies of both Mo $3d_{5/2}$ and Mo $3d_{3/2}$ increased initially and decreased afterwards with increasing the annealing temperature, and the peak binding energies were obtained at the temperature of 473 K. It is suggested that the relative amount of Mo^{5+} decreased while the annealing

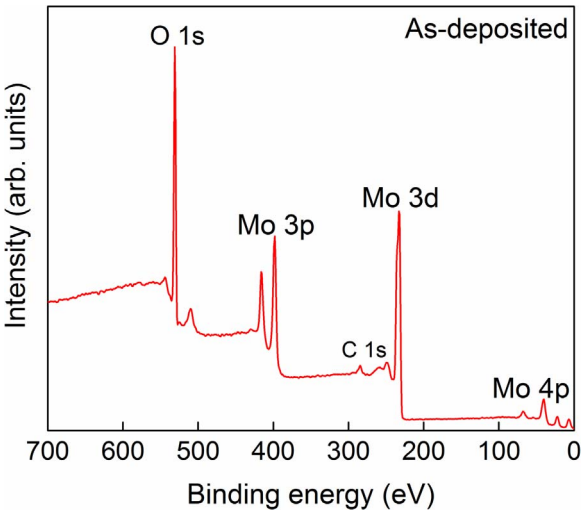

Fig. 1. XPS survey scan spectrum of as-deposited MoO_x film.

Table 1
Electronic binding energies of as-deposited MoO_x film.

Peak name	Peak position (eV)	Peak name	Peak position (eV)
O 1s	530.79	Mo $3d_{5/2}$	232.88
Mo $3p_{3/2}$	398.08	Mo $3d_{3/2}$	235.98
Mo $3p_{1/2}$	416.08	Mo 4p	39.08
C 1s	284.88	O 2s	22.00

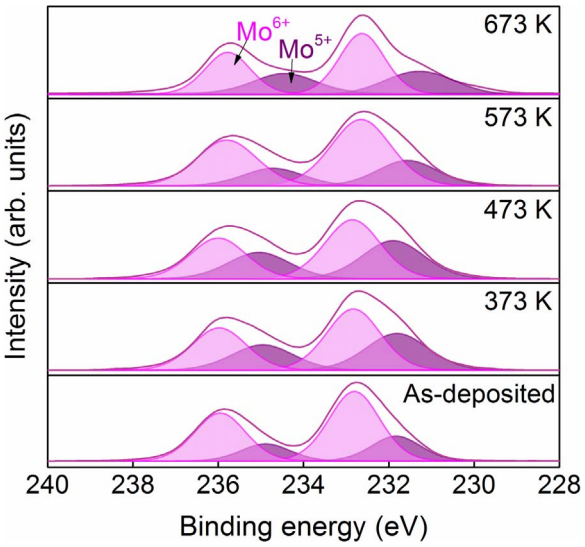

Fig. 2. XPS electronic binding energy of Mo 3d doublets of MoO_x films annealed at various temperatures.

Table 2
Electronic binding energy of molybdenum and oxygen in MoO_x films, as well as the ratio of oxygen to molybdenum.

Annealing temperature (K)	Binding energy (eV)					Ratio O/Mo
	Mo^{6+}		Mo^{5+}		O 1s	
	Mo $3d_{5/2}$	Mo $3d_{3/2}$	Mo $3d_{5/2}$	Mo $3d_{3/2}$		
As-deposited	232.81	235.96	231.72	234.87	530.82	2.58
373	232.83	235.98	231.81	234.96	530.82	2.63
473	232.85	236.00	231.90	235.05	530.87	2.75
573	232.65	235.80	231.57	234.72	530.78	2.56
673	232.63	235.78	231.30	234.45	530.40	2.37